

## Orthogonal frequency division multiplexing for improving the performance of terahertz channel

M. Bharathi , A. Amsaveni , S. Sasikala

( Kumaraguru College of Technology , Coimbatore 641049 , India)

**Abstract:** Terahertz ( THz) communication is considered to be one of the demanding technology for the upcoming 5G standards. The incredible demand for high rate through wireless channel necessitates the use of THz frequency for communication. The development of communication systems in this frequency band possess technical challenges as the characteristic of THz band is very different from the present wireless channel. However ,the advancements in the development of transceiver and antenna systems are rapidly bringing the THz communication into reality. The high path loss in THz band limits the communication range of this channel. Even ,for a distance of few meters ( > 5 m) , the absorption coefficient is very high and hence the performance of the system is poor. Performance over this frequency channel can be enhanced by considering transmission windows over this band instead of the entire band. The transmission windows are the frequencies over which the absorption is relatively low. Though there is an improvement in the performance with this adaptive modulation scheme ,but not sufficient for longer distance. Apart from path loss ,the frequency selective nature of this high bandwidth channel is also a major reason for the poor performance of THz channel. Orthogonal Frequency Division Multiplexing ( OFDM) is a promising solution to mitigate the effects of frequency selective nature of the wireless channel. OFDM has been exploited in this paper to improve the performance of terahertz channel. The results show that the Bit Error Rate ( BER) of the terahertz channel is considerably improved with OFDM.

**Key words:** terahertz communication , channel modeling , LOS , NLOS , performance , BER , OFDM

**PACS:** 89. 70. Cf , 89. 70. Kn

### Introduction

Current digital age demands speedy transmission of large amounts of data which needs the evolution of new wireless technologies<sup>[1]</sup>. Advanced modulation schemes and signal processing techniques in the physical layer increased the spectral efficiency of the current wireless communication systems<sup>[2,3]</sup>. However , the spectrum scarcity of the present day communication systems put an upper bound for the achievable data rates. THz communication is envisioned as a key technology to overcome the spectrum scarcity<sup>[1-4]</sup>. THz frequencies has shorter wavelengths than microwaves and therefore has higher bandwidth capacity for data transmission ranging from tens of GHz up to several THz depending on the transmission distance. The available bandwidth is more than one order of magnitude above the mm-Wave systems. Terabit-per-second ( Tbps) data rate is achieved using this high bandwidth channel. Terahertz radiation provides a more focused signal that could improve the efficiency of commu-

nication stations and reduce power consumption of mobile towers. Communication over this ultra-broadband channel possesses novel communication challenges such as propagation modelling , capacity analysis , modulation schemes , and other physical and link layer solutions<sup>[1]</sup>. However , the advancements in the development of transceiver and antenna systems are rapidly bringing the THz communication into reality<sup>[4-6]</sup>. THz band will facilitate a range of application starting from high speed 5G communication to Nano networks. Nano networks include diversified range of applications from healthcare to home security. The feasibility of THz communication for WLAN application is explored in Ref. [7]. The usefulness of THz communication in Nano networks has been highlighted in Ref. [1-6].

THz waves ranges from 0. 1 to 10 Terahertz and the corresponding wavelength from 3 000 to 30  $\mu\text{m}$ <sup>[1,3]</sup> are highly absorbed by water vapors present in the atmosphere. The communication distance is limited because of this high absorption. Model of both LOS and NLOS paths in THz frequency have been researched extensively in the recent past. LOS propagation model for the THz band

**Received date:** 2018-08-21 , **revised date:** 2018-12-22

**收稿日期:** 2018-08-21 , **修回日期:** 2018-12-22

**Foundation items:** NIL Research Found of Department of Electronics and Communication Engineering , Kumaraguru College of Technology , Coimbatore , India

**Biography:** M. Bharathi , female , Professor , Research areas includes communication , signal processing. Email: bharathi. m. ece@kct. ac. in

\* **Corresponding author:** E-mail: bharathi. m. ece@kct. ac. in

was developed and analyzed in Ref. [8, 9]. Molecular absorption and spreading loss are the major factors in LOS path. The model of NLOS path must account for the reflection of electromagnetic waves at obstacle [10]. The reflection characteristics depend on the material<sup>[11-12]</sup>. In Ref. [9, 13] the multipath THz channel including LOS and NLOS propagation paths has been developed using raytracing simulation. The capacity of the THz channel considering a single transmission window of almost 10 THz wide has been investigated in Ref. [8]. With increase in distance, performance degrades rapidly due to high absorption loss. To overcome this, adaptive modulation schemes has been proposed<sup>[14]</sup>, where transmission windows are used for transmission instead of entire band. As the highly attenuated frequencies are not used in adaptive modulation scheme, this improves the performance of the channel. But this also limits the distance to less than 5 m.

In wireless system, multiple antennas are used to accomplish a multiplexing gain, a diversity gain, or an antenna gain, thus enhancing the bit rate, the error performance, or the signal-to-noise-plus-interference ratio respectively<sup>[17, 18]</sup>. Conventional single-antenna system obtains optimal performance by exploiting the time domain and/or the frequency domain. Employing multiple antennas, exploits the spatial domain to maximize the system performance. In Ref. [15], multipath channel for THz band is developed and the performance of the channel is analyzed with BPSK modulation scheme over selected transmission windows. To improve the performance for distance > 5m, receive diversity techniques<sup>[20]</sup> with Maximal Ration combining (MRC) have been used along with adaptive BPSK modulation. However, with MIMO the complexity of the system increases.

Data transmission over a high bandwidth channel will make the channel frequency selective which causes Inter Symbol interference (ISI) and hence wide band data transmission through wireless channel is a challenging task. Orthogonal Frequency Division Multiplexing (OFDM) is the widely accepted multicarrier signal processing technique suitable for wide band data transmission. Multicarrier techniques can combat hostile frequency-selective fading encountered in wireless communications. The robustness of OFDM against frequency selective fading is very attractive, especially for high-speed data transmission. OFDM technique converts the frequency selective channel into flat fading channels that avoids the use of equalizers<sup>[21, 22]</sup>. It uses a large number of closely separated orthogonal sub-carriers that are transmitted in parallel. Each of the sub-carrier is modulated with any conventional digital modulation scheme. In this paper the performance of ultra-band width THz channel is analyzed with OFDM.

Section II of this paper describes LOS and NLOS channel modeling. The performance analysis of THz channel using BPSK and adaptive BPSK is studied in Section III. Section IV discusses the performance of THz channel with diversity techniques. OFDM with adaptive modulation for enhancing the performance of THz channel is introduced and analyzed in Section V. Concluding Remarks are highlighted in section VI.

## 1 Channel Modeling

THz wireless channel consists of both Line of Sight (LOS) propagation path and Non Line of Sight (NLOS) propagation paths. To model the THz channel both LOS and NLOS paths has to be modeled. LOS path is highly influenced by the molecular absorption which is a strong function of the gas molecules present in the atmosphere. The gas molecules resonate in this frequency range and absorb the signal energy propagating through them<sup>[1-3]</sup>. The absorption coefficient of different gas molecules in the atmosphere can be computed using the High Resolution Transmission (HITRAN) data base. HITRAN is a compilation of spectroscopic parameters used to predict and simulate the transmission, absorption and emission of light through gaseous media<sup>[16]</sup>. Absorption coefficient is also a function of frequency, temp and pressure. Figure 1 shows absorption coefficient as a function of wavenumber starting from 3.3 cm<sup>-1</sup> to 50 cm<sup>-1</sup> (0.1 THz to 1.5 THz) for two different temperatures 293-degree Kelvin (20°C) and 303 (30°C) degree Kelvin. Pure water vapor is considered as the atmospheric gas. Absorption coefficient is slightly higher for lower temperature but they follow a similar pattern for both temperatures peaking at some frequencies. Absorption peaks occurs at wave numbers 19 cm<sup>-1</sup>, 25 cm<sup>-1</sup>, 33 cm<sup>-1</sup>, 37-42 cm<sup>-1</sup> and 47 cm<sup>-1</sup> corresponds to frequency 0.55 THz, 0.74THz, 0.98 THz, 1.09 to 1.25 THz and 1.41THz.

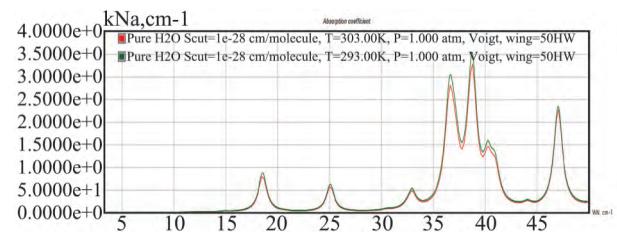


Fig. 1 Absorption coefficient of water vapor

The absorption loss of the electromagnetic wave with frequency propagating over a distance is<sup>[9]</sup>

$$A_{abs}^{dB}(f, r) = \alpha_{mol}(f, T, p) r 20 \log e \quad (1)$$

As electromagnetic waves propagate through the medium it gets expanded which results in spreading loss. Spreading loss depends on the distance and is defined as

$$A_{spread}^{dB}(f, r) = 20 \log_{10} \frac{(4\pi fr)}{c} \quad (2)$$

where,  $c = 2.9979 \times 10^8$  m/s is the speed of light.

The total LOS path loss is the result of both absorption loss and spreading loss and is given as

$$A_{dB}(f, r) = A_{abs}^{dB}(f, r) + A_{spread}^{dB}(f, r) \quad (3)$$

LOS path loss as a function of frequency for various distance is given in Figure 2(a) and 2(b) for 20°C Celsius and 30°C Celsius respectively. Path loss is highly frequency-selective and is 100 dB even for a distance of few meters. Depending on the distance and the composition of the gas mixture in the atmosphere, at some frequencies the path loss is too high. This high path loss in certain frequencies forms transmission windows<sup>[14]</sup>.

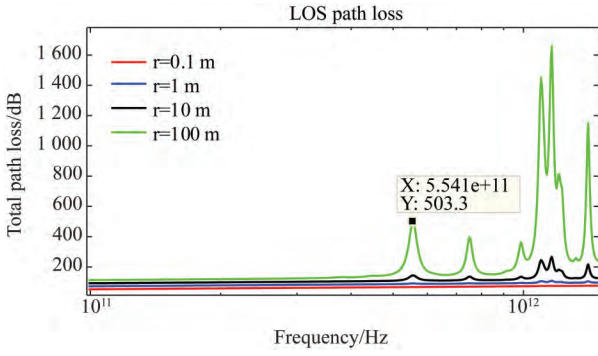


Fig.2 (a) LOS Path Loss for 20°C Celsius

The transfer function of the LOS propagation path is given by ,

$$H^{LOS}(f,r) = H_{spread}(f,r) \cdot H_{abs}(f,r) \quad (4)$$

Where ,  $H_{spread}(f,r) = c/4\pi fr$  and

$$H_{abs}(f,r) = e^{-\frac{1}{2} \alpha_{mol}(f,T_k \Phi) r}$$

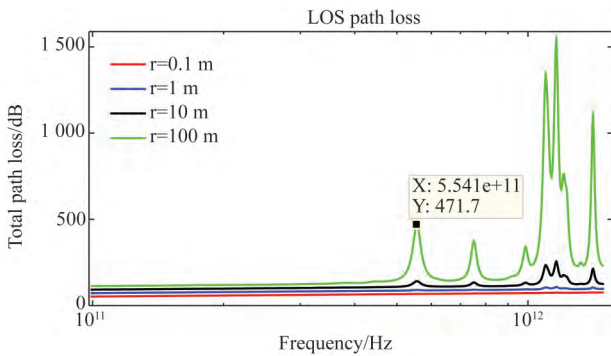


Fig.2 (b) LOS Path Loss for 30°C Celsius

Non Line of Sight ( NLOS ) path in THz system plays a major role in enabling communication in the scenario where the LOS path is blocked by obstacles like walls and furniture. Path loss in NLOS path depends mainly on the reflection of the electromagnetic waves. Hence , it is necessary to analyze the reflection properties of the surface which depends on the building material such as roughness of the surface , and correlation length<sup>[11]</sup>. The scattering of the EM waves at rough surfaces is employed by means of Kirchhoff scattering theory<sup>[12]</sup>. Scattering coefficient determines the nature of reflected wave<sup>[9]</sup> and is given by ,

$$\rho = \frac{E_{sc}}{E_{ref}} \quad (5)$$

where ,  $E_{sc}$  is the scattered electric field and  $E_{ref}$  is the reflected electric field in the direction of specular reflection by a smooth conducting surface. In specular reflection , the incident angle  $\theta_1$  and the reflected angle  $\theta_2$  are equal and hence scattering angle  $\theta_3$  , in direction outside the plane of incidence equals to zero<sup>[9]</sup>.

For an infinitely conductive surface of area A with dimension X and Y , the mean value of the scattering coefficient with incident angle  $\theta_1$  and the scattered angles  $\theta_2 \theta_3$  is derived as ,

$$E\{\rho\rho^*\}_\infty = e^{-g} \left( \rho_o^2 + \frac{\pi l_{corr}^2 F^2}{A} \sum_{m=1}^{\infty} \frac{g^m}{mm!} e^{-v_y^2} l_{corr} 2l(vm) \right) \quad (6)$$

where ,  $g = \sigma_{hs}^2 (2\pi f/c)^2 (\cos\theta_1 + \cos\theta_2)^2$   
 $\rho_o = \text{sinc}(v_x X) \cdot \text{sinc}(v_y Y)$   
 $v_x = (2\pi f/c) (\sin\theta_1 - \sin\theta_2 \sin\theta_3)$   
 $v_y = (2\pi f/c) (-\sin\theta_2 \sin\theta_3)$   
 $v_{xy} = \sqrt{v_x^2 + v_y^2}$   
 $F = \frac{1 + \cos\theta_1 \cos\theta_2 - \sin\theta_1 \sin\theta_2 \cos\theta_3}{\cos\theta_1 (\cos\theta_1 + \cos\theta_2)}$

Equation (6) is applicable for perfect conducting surface. Furthermore , the average scattering coefficient for finite conducting surface is computed by average the Fresnel reflection coefficient with scattering coefficient of the infinite conducting surface<sup>[11,12]</sup>.

$$E\{\rho\rho^*\}_{finite} = E\{\rho\rho^*\}_\infty E\{\gamma\gamma^*\} \quad (7)$$

For the finite conducting surface , the Fresnel reflection coefficient for the air and the material interface is computed by ,

$$\gamma = \frac{1 - \eta_{eff}}{1 + \eta_{eff}} \quad (8)$$

By considering all the derived equations , the scattered power with respect to the distance is given by ,

$$E\{R_{power}\} = \left( \frac{fA \cos\theta_1}{cr_0} \right)^2 E\{\rho\rho^*\}_{finite} \quad (9)$$

The transfer function of the  $i^{th}$  NLOS path is

$$H_i NLOS(f,r,\xi_i) = H_{ref,i}(f,r_{i2},\theta_{i1},\theta_{i2},\theta_{i3}) \times H_{spread,i}(f,r_{i1},r_{i2}) \cdot H_{abs,i}(f,r_{i1},r_{i2}) \quad (10)$$

where  $H_{ref,i}(f,r_{i2},\theta_{i1},\theta_{i2},\theta_{i3}) = \sqrt{E\{R_{power,i}(f,r_{i2},\theta_{i1},\theta_{i2},\theta_{i3})\}}$

$$H_{spread,i}(f,r) = \frac{4\pi f (r_{i1} + r_{i2})}{c}$$

$$H_{abs,i}(f,r_{i1},r_{i2}) = e^{-\frac{1}{2} \alpha_{mol}(f,T_k \Phi)(r_{i1} + r_{i2})}$$

$r$  the distance between the transmitter and receiver  
 $r_{i1}$  the distance between the transmitter and the scattering point  
 $r_{i2}$  is the distance between the scattering point and the receiver.

The overall channel transfer function considering both LOS and NLOS paths is given by

$$HEQ(f,r,\zeta) = H^{LOS}(f,r) e^{-2\pi f \tau_{LOS}} + \sum_{i=1}^N H_i NLOS(f,\zeta_i) e^{-2\pi f \tau_{NLOS_i}} \quad (11)$$

The vector  $\zeta = [\zeta_1, \zeta_2, \dots, \zeta_N]$  is coordinates of all the scattering points , which accounts for the parameters  $[r_{i1}, r_{i2}, \theta_{i1}, \theta_{i2}, \theta_{i3}]$ . N is the total number of NLOS paths.

In this paper , a rectangular room of ( length ,width , height ) = ( 5 m 2.75 m 2.5 m ) with four NLOS paths is considered for simulation and is shown in Figure 3. The simulated LOS channel transfer function , NLOS channel transfer function and the complete transfer functions for a distance of 2m at 30°C Celsius are given in Figure 4. From the result it is clear that in the presence of LOS path it dominates the NLOS path and the complete transfer function can be approximated as LOS path transfer function.

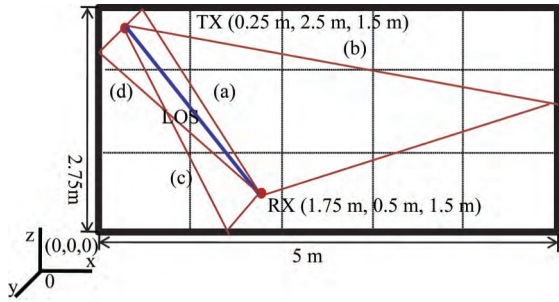


Fig. 3 Indoor scenario

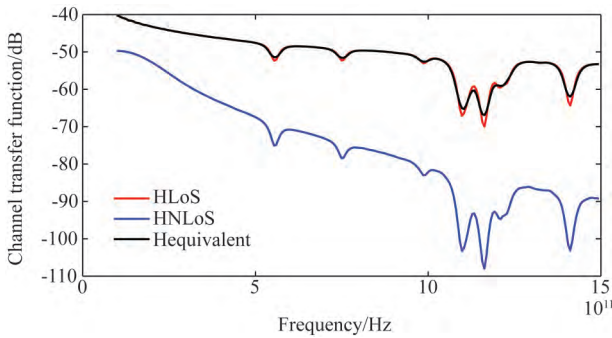


Fig. 4 Channel transfer function

## 2 Performance of THZ Channel with Adaptive BPSK

Binary Phase Shift Keying (BPSK) modulation scheme is used over THz channel and the Bit Error Rate (BER) performance for different length of the channel is calculated. BPSK is a digital modulation technique in which each bit is encoded with a phase shift over a predetermined period. Performance of THz channel of different length with BPSK modulation scheme is given in Figure 5. Frequency range from 0.1THz to 1.2 THz is been considered for simulation.

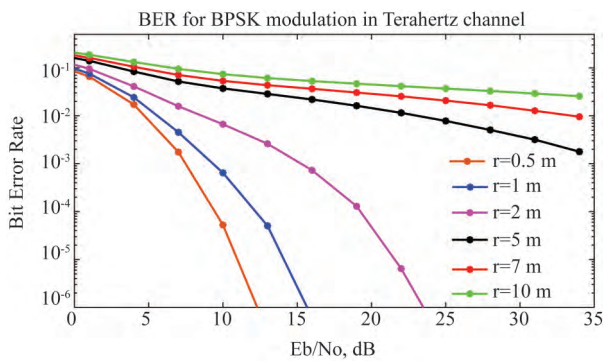


Fig. 5 BER performance of THz channel with BPSK modulation

Performance of the channel is considerably good for the distance of 0.5 m and 2 meters. As the distance increases, due to the high absorption coefficient and fre-

quency selective nature of the channel the performance degrades. Even with high SNR the noise floor dominates the signal and the performance is poor.

The characteristic and limitation of the channel can be exploited to improve the performance of the system. Frequency selective abortion of water molecules absorbs more signal in some frequencies and this results in attenuation bands. The information passed over these band of frequencies are more suffered. The width of these high attenuation bands mainly depends on the distance and humidity in the air. In adaptive modulation these high attenuation bands are excluded from data transmission. The rate of transmission using adaptive modulation decreases but improves the BER performance<sup>[14]</sup>. Figure 6 shows the performance of the system with adaptive modulation scheme. Frequency bands of 0.5-0.6 THz, 0.7-0.78 THz, 0.93-0.98 THz and 1.09-1.2 THz are found to be high attenuation bands and are not considered for data transmission. With adaptive modulation, there is a 15 dB gain for 5m distance and 20 dB gain for 10m distance. However, even with this improvement the quality of data transmission is not sufficient.

## 3 Performance of THZ Channel with MIMO

The space dimension is exploited in Multi-Input Multi-Output (MIMO) technique to improve capacity, range and reliability of data transmission. In MIMO multiple co-located antennas are used either at the transmitter or at the receiver or at both the ends for enhancing the performance. This spatial diversity schemes enhance reliability by minimizing the channel fluctuations due to fading. The central idea in diversity is that different antennas receive different versions of the same signal. The chances of all these copies being in deep fade are small<sup>[17]</sup>. Receiver diversity is a form of space diversity, where there are multiple antennas at the receiver as shown in Figure 7.

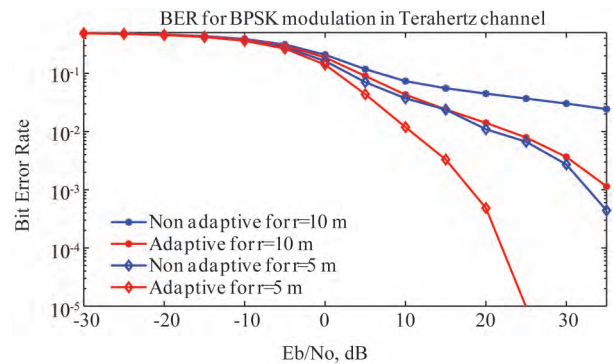


Fig. 6 BER performance of THz channel with adaptive BPSK

The received signal in the  $i^{th}$  received antenna is given by

$$y_i = h_i x + n_i \quad , \quad (12)$$

In matrix form,

$$Y = HX + N \quad , \quad (13)$$

where  $Y = [y_1 \ y_2 \ \dots \ y_{N_r}]^T$  is the received signal from all the received antenna

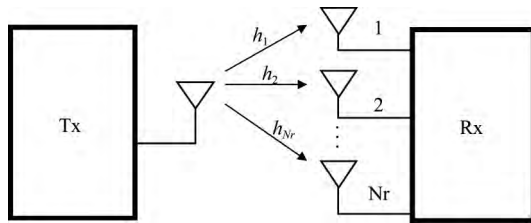


Fig. 7 Schematic of Receiver diversity

$$H = [h_1 \ h_2 \ \dots \ h_{N_r}]^T \text{ is the channel for the antennas}$$

$$N = [n_1 \ n_2 \ \dots \ n_{N_r}]^T \text{ is the noise on the received signal}$$

nal

Different combining techniques are used to effectively demodulate the data using the information from all antennas. In this paper, Maximum Ratio Combining (MRC) is used to estimate the data as this is optimal in terms of SNR<sup>[20]</sup>. The estimated symbol is obtained by,

$$\hat{x} = \frac{H^H Y}{H^H H} \quad (14)$$

Adaptive BPSK modulation with receiver diversity is used and the performance of the channel is obtained. For different number of receive antenna the performance of the channel for both 5m and 10m distance is obtained and is shown in Figure 8. For 5m distance there is a 15 dB gain and for 10m distance there is 12 dB gain with 32 antennas compared to 2 antenna system. However, the complexity and the size of the Transmitter and receiver increases with number of antennas.

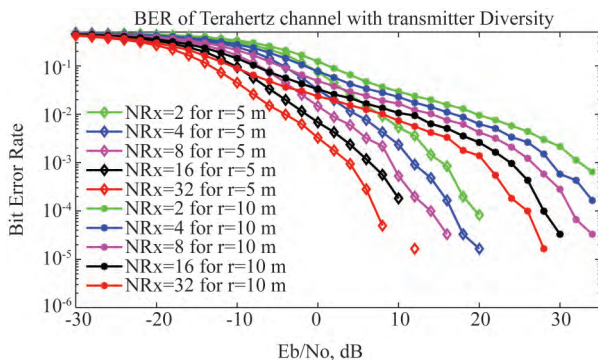


Fig. 8 BER performance of THz channel with MIMO

#### 4 Performance of THz Channel with OFDM

Orthogonal frequency division multiplexing (OFDM) is a promising technique for high-data-rate wireless communications because it can combat inter-symbol interference (ISI) caused by the dispersive fading of wireless channels. In wideband wireless data transmission, the symbol duration becomes smaller than the delay spread of the channel. This results in Inter Symbol Interference (ISI) and severely degrades the system performance. To mitigate the effect of ISI, adaptive equalizer can be used at the receiver. However, it needs high computational power to update the equalizer and training at regular intervals which would reduce the spectral efficiency of the

system. Also it is not an attractive solution as the time latency is a major issue. OFDM is a special type of Multi carrier modulation technique which provides high bandwidth efficiency by allowing the sub channels to overlap. Improved immunity against multipath effect is one of the major advantages of OFDM.

OFDM converts wideband data into parallel stream of narrow band data<sup>[21]</sup>. The narrow band parallel data makes the channel flat and removes the problem of frequency selective nature of wideband channel. The low rate OFDM signal is wide enough to make the ISI negligible. To implement the narrow parallel streams, the input data is demultiplexed and transmitted through separate subcarriers. The block diagram of OFDM used for THz band is shown in Figure 9. The total number of subcarriers are  $N$ . A block of number of BPSK modulated signal is taken ( $X = [X(0) \ X(1) \ \dots \ X(N-1)]$ ) and Inverse Fourier Transform is computed for this block. This parallel data stream is converted to serial data  $x(n)$  using a parallel to serial converter.

$$x(n) = \frac{1}{N} \sum_{k=0}^{N-1} X(k) e^{j \frac{2\pi}{N} kn} \quad n = 0, 1, N-1 \quad (15)$$

Cyclic prefix is added along with OFDM symbol. This is performed by adding  $L$  samples from the tail of the OFDM block to the front. The cyclic prefixed OFDM signal  $u(n)$  is

$$u(n) = [x(N-L) \dots x(N-1), x(0), x(1), \dots, x(N-1)] \quad (16)$$

After the addition of cyclic prefix, the length of the OFDM block will be equal to  $N + L$ . Addition of cyclic prefix helps in avoiding Inter Block Interference (IBI) and also this results in a circular convolution at the receiver. At the receiver, the received signal  $y$  is given by

$$y = x \otimes h \quad (17)$$

The cyclic prefix is removed at the receiver and at the output of the FFT block the signal is

$$Y(k) = X(k) H(k) \quad (18)$$

Knowing the channel state information,  $X(k)$  can be estimated ( $\hat{X}(k)$ ) and the parallel to serial converter gives the estimated signal.

The performance of the THz channel with OFDM and adaptive BPSK is shown in Figure 10. There is a 10 dB gain in SNR with OFDM and adaptive modulation compared to adaptive modulation over the entire block as a whole. The performance of OFDM with single receive antenna (Figure 10) is equivalent to having 32 receive antennas (Figure 8) for 5m and 8 receive antenna for 10 m. Using OFDM, the performance of the channel is improved with less transceiver complexity.

#### 5 Conclusion

THz communication is one of the promising solution to satisfy the demand for high data rate over wireless channel. This paper, gives an overview of LOS and NLOS channel model for THz frequency. The performance of the channel is analyzed with BPSK and adaptive BPSK modulation technique. Even with adaptive modulation, the BER performance of the channel is poor for distance  $> 5$  m. Multiple input multiple output (MIMO) improves the performance of the system however the com-

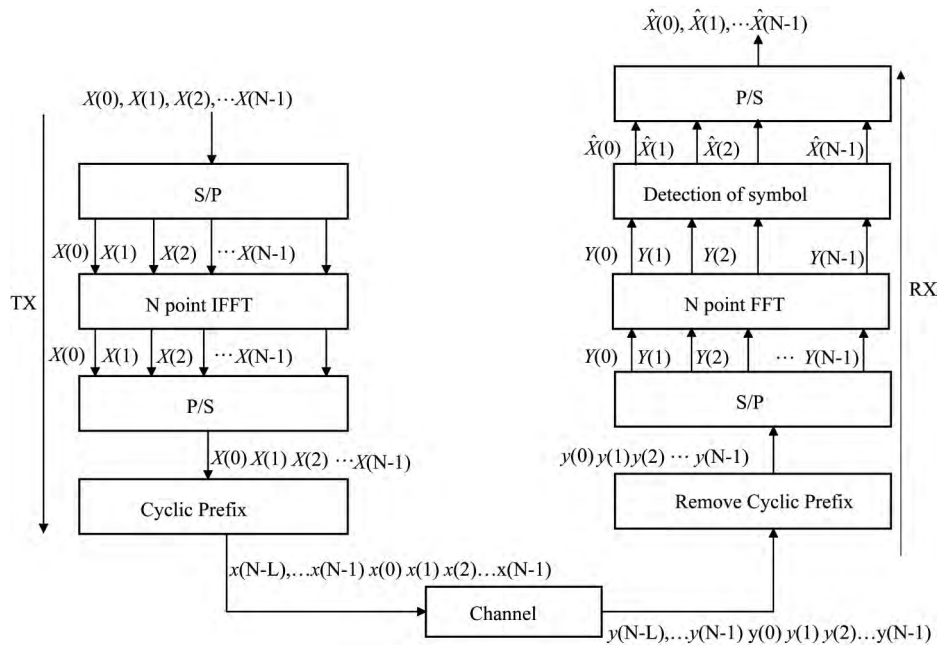


Fig. 9 Tx-Rx Schematic of OFDM

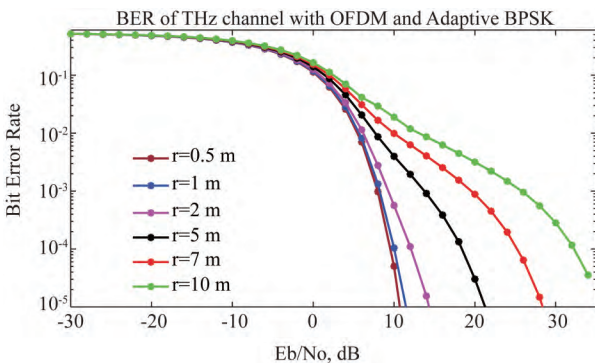


Fig. 10 The BER performance of THz channel OFDM

plexity also increases with the number of antennas. OFDM is the multicarrier modulation technique employed to mitigate the effect of ISI in wideband channels. In this paper OFDM for THz frequency band is explored with adaptive BPSK modulation and the performance is evaluated. The result shows there is 10dB gain in SNR with OFDM compared to considering the band as a whole.

References

[1] I. Akyildiz, J. Jornet, C. Han. Terahertz band: Next frontier for wireless communications [J]. Physical Communication, 2014, 12: 16-32.  
 [2] H. Song, T. Nagatsuma. Present and future of terahertz communications (J). IEEE Transactions on Terahertz Science and Technology, 2011, 1(1): 256-263.  
 [3] Thomas Kurner, Sebastian Priebe. Towards THz Communications-Status in Research, Standardization and Regulation (J). Journal Infrared Milli and Terahz Waves, 2014, 35(1): 53-62.  
 [4] Ian F. Akyildiz, Josep Miquel Jornet, Chong Han. Teranets: Ultra-Broadband Communication Network in the Terahertz Band (J). IEEE Wireless Communications, 2014, 21(4): 130-135.  
 [5] Akkihiko Hirata, Makoto Yaita. Ultrafast Terahertz Wireless Communications Technologies (J). IEEE Transaction on Terahertz Science and

Technology, 2015, 5(6): 1128-1132.  
 [6] Turker Yilmaz, Ozgur B. Akan. On the 5G Wireless Communications at the Low Terahertz Band [J/OL]. https://arxiv.org/pdf/1605.02606.pdf.  
 [7] Yonghoon Choi. Performances and Feasibility of THz Indoor Communication for Multi-Gigabit Transmission [C]. P. First International Conference on Artificial Intelligence, Modelling & Simulation, 2013: 400-404.  
 [8] Josep Miquel Jornet, Ian F. Akyildiz. Channel Modeling and Capacity Analysis for Electromagnetic Wireless Nanonetworks in the Terahertz Band [J]. IEEE Transaction on Wireless Communication, 2011, 10(10): 3211-3221.  
 [9] Anamaria Moldovan, Michael A. Ruderl, Ian F. Akyildiz, Wolfgang H. Gerstacker. LOS and NLOS Channel Modeling for Terahertz Wireless Communication with Scattered Rays [C]. P. Globecom Workshop Mobile Communication in Higher Frequency Bands, 2014: 388-392.  
 [10] Radoslaw Piesiewicz, Martin Jacob, Thomas Kurner. Overview of challenges in channel and propagation characterization beyond 100 GHz for wireless communication systems [J/OL]. 2008.  
 [11] R. Piesiewicz, C. Jansen, S. Wietzke, D. Mittleman, M. Koch, T. Kürner. Properties of building and plastic materials in the THz range [J]. International Journal of Infrared and Millimeter Waves, 2007, 28(5): 363-371.  
 [12] R. Piesiewicz, C. Jansen, D. Mittleman, T. Kleine-Ostmann, M. Koch, T. Kürner. Scattering analysis for the modeling of THz communication systems [J]. IEEE Transactions on Antennas and Propagation, 2007, 55(11): 3002-3009.  
 [13] Joonas Kokkonen, Janne Lehtomaki, Kenta Umabayashi, Markku Juntti. Frequency and Time Domain Channel Models for Nanonetworks in Terahertz Band [J]. IEEE Truncation on Antenna and Propagation, 2015, 63(2): 678-691.  
 [14] Farnoosh Moshir, Suresh Singh. Pulsed Terahertz Time-Domain Communication [C]. P. Globecom Wireless Communication Symposium, 2014: 3796-3801.  
 [15] M. Bharathi, S. Sasikala, Vanmathi J. Performance Analysis of Terahertz Channel with Multiple Input Multiple Output Techniques, Journal of infrared and millimeter waves 2017, 36(6): 641-645.  
 [16] L. Rothman, I. Gordon, Y. Babikov, et al., The HITRAN 2012 molecular spectroscopic database [J]. Journal of Quantitative Spectroscopy and Radiative Transfer, 2013, 130: 4-50.

(下转第 284 页)

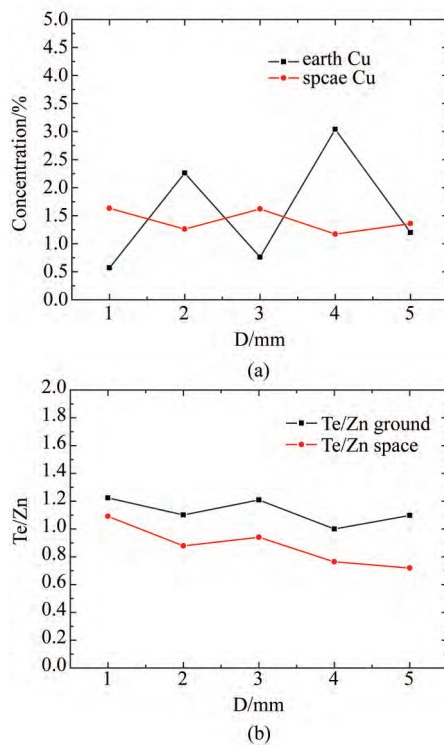


Fig. 6 Comparison of radial compositional uniformity distribution of space and ground samples  
图 6 空间和地面样品纵向组分分析

ter than 1, serious Te segregation in the ground sample indicates that the microgravity environment is effective to the reduction of Te inclusions.

The crystalline of space crystal are better than that of the ground crystals. The space sample with a size of

10 mm × 6 mm × 2 mm crystal in the final condensation area is larger than the ground sample with a size of 3 mm × 3 mm × 1 mm crystal. The results have shown that the microgravity condition is preferable to the growth of II-VI semiconductor materials.

## References

- [1] Jun Shao. Optical and magneto-optical study of ZnTe:  $Ti_3 + [D]$ . Physikalisches Institut der Universität Stuttgart, 2001.
- [2] V. I. Kozlovsky, A. B. Krysa, Yu. V. Korostelin, MBE growth and characterization of ZnTe epilayers and ZnCdTe/ZnTe structures on GaAs(1 0 0) and ZnTe(1 0 0) substrates [J]. *Journal of Crystal Growth* 2000: (214/215) 35-39.
- [3] ZHAO Jiaohua, WANG Wenkui, Research Progress in the Crystal from Vapor Phase in Space [J]. *Progress in Physics*, 1998, **18**(3): 283-307.
- [4] E. B. Borisenko, N. N. Kolesnikov, A. S. Senchenkov, M. Fiedlerle, Crystal growth of  $Cd_{1-x}Zn_xTe$  by the traveling heater method in microgravity onboard of Foton-M4 spacecraft [J]. *Journal of Crystal Growth*. 2017, (457) 262-264.
- [5] Mikito Mamiya\*, Hideaki Ngai, Martin Castillo, et al. The analysis of CdTe solidification in absence of thermal convection via short-duration microgravity [J]. *Journal of Crystal Growth*, 2006, (295): 209-216.
- [6] Croll A, Kaiser T, Schweizer A N. Floating-zone and floating-solution-zone growth of GaSb under microgravity [J]. *Journal of Crystal Growth*, 1998, (191): 365.
- [7] WANG Reng, LI Xiangyang, LU Ye. Research of CdZnTe crystal Vapor growth under Microgravity [J]. *Infrared*, 2013, **34**(11): 8-12.
- [8] Wang Reng, Li Xiangyang. Characterization of CdZnTe crystal using THz time-domain spectroscopy [J]. SPIE 2012.
- [9] LU Ye, WANG Reng, et al. Growth of ZnTe crystal in microgravity on Tiangong-2 spaceship (in Chinese) [J]. *Chin. J. Space Sci.* 2018, **38**(2): 234-238.
- [10] WANG Reng, LU Ye, et al. Cathodoluminescence characterization analysis and growth of ZnTe: Cu under Microgravity (in Chinese) [J]. *J. Infrared Millim. Waves*, 2018, **2**(1): 47-49.
- [11] Wang Reng, LU Ye, et al. Growth of ZnTe crystal in microgravity on Tiangong-2 spaceship (in Chinese) [J]. *Chin. J. Space Sci.* 2018, **38**(2): 234-238.
- [12] Wang Reng, LU Ye, et al. Cathodoluminescence characterization analysis and growth of ZnTe: Cu under Microgravity (in Chinese) [J]. *J. Infrared Millim. Waves*, 2018, **2**(1): 47-49.
- [13] Wang Reng, LU Ye, et al. Cathodoluminescence characterization analysis and growth of ZnTe: Cu under Microgravity (in Chinese) [J]. *J. Infrared Millim. Waves*, 2018, **2**(1): 47-49.
- [14] Wang Reng, LU Ye, et al. Cathodoluminescence characterization analysis and growth of ZnTe: Cu under Microgravity (in Chinese) [J]. *J. Infrared Millim. Waves*, 2018, **2**(1): 47-49.
- [15] Wang Reng, LU Ye, et al. Cathodoluminescence characterization analysis and growth of ZnTe: Cu under Microgravity (in Chinese) [J]. *J. Infrared Millim. Waves*, 2018, **2**(1): 47-49.
- [16] Wang Reng, LU Ye, et al. Cathodoluminescence characterization analysis and growth of ZnTe: Cu under Microgravity (in Chinese) [J]. *J. Infrared Millim. Waves*, 2018, **2**(1): 47-49.
- [17] Jan Mietzner, Robert Schober, Lutz Lampe, Wolfgang H. Gerstacker, Peter A. Hoeher. Multiple-Antenna Techniques for Wireless Communications-A Comprehensive Literature Survey [J]. *IEEE Communication Surveys and tutorials*, 2009, **11**(2): 87-105.
- [18] Mehul. R. Amin, Sammer. D. Trapasiya. Space Time Coding Scheme for MIMO System-Literature Survey [J]. *Procedia Engineering*, 2012: 3509-3517.
- [19] Siavash M. Alamouti. A Simple Transmit Diversity Technique for Wireless Communications [J]. *IEEE Journal on Selected Areas in Communication*, 1998, **16**(8): 1451-1458.
- [20] Zhuo Chent, Branka Vucetid, Jinhong Yuan, Ka Leong Lot. Analysis of Transmit Antenna Selection/ Maximal-Ratio Combining in Rayleigh Fading Channels [C]. P. International Conference on Communication Technology, 2003: 1532-1536.
- [21] Prasad, R 2004, OFDM for Wireless Communications Systems, Artech House Inc., Boston, London.
- [22] Hermann Rohling, OFDM Concepts for Future Communication Systems, Springer, 2011.

(上接第 268 页)

- [17] Jan Mietzner, Robert Schober, Lutz Lampe, Wolfgang H. Gerstacker, Peter A. Hoeher. Multiple-Antenna Techniques for Wireless Communications-A Comprehensive Literature Survey [J]. *IEEE Communication Surveys and tutorials*, 2009, **11**(2): 87-105.
- [18] Mehul. R. Amin, Sammer. D. Trapasiya. Space Time Coding Scheme for MIMO System-Literature Survey [J]. *Procedia Engineering*, 2012: 3509-3517.
- [19] Siavash M. Alamouti. A Simple Transmit Diversity Technique for Wireless Communications [J]. *IEEE Journal on Selected Areas in Commu-*